JOURNAL OF AIRCRAFT
Vol. 30, No. 6, Nov.–Dec. 1993

Target Pitch Angle for the Microburst Escape Maneuver

Sandeep S. Mulgund* and Robert F. Stengel†
Princeton University, Princeton, New Jersey 08544

Commuter and general aviation aircraft face no less a threat from microburst wind shear than do large jet transport aircraft, yet the majority of flight dynamic research has emphasized recovery performance and piloting techniques for jet transport aircraft. The current work investigates the effects of microburst wind shear on propeller-driven commuter-type aircraft. Recovery performance of a commuter-type aircraft in a microburst encounter is examined using a constant-pitch-attitude strategy and flight path optimization. The goals are to identify a suitable target pitch angle for the escape maneuver and to determine the nature of an optimal escape maneuver for a commuter-type aircraft. The results demonstrate that the pitch attitude which maximizes climb rate in a wind shear condition is strongly dependent on whether the aircraft is subjected to a horizontal shear or a downdraft. Simulated constant-pitch-attitude recoveries through an analytic downburst model show that the pitch attitude which maximizes ground clearance, depends on the altitude of the encounter, the strength of the microburst, and the initial position of the aircraft with respect to the downburst core. In severe wind shear encounters at very low altitudes, best results are obtained at relatively low-target pitch angles (TPA). Excessively high-target pitch angles subject the aircraft to prolonged periods at stall warning angle of attack. The flight path optimization demonstrates that a technique which maximizes ground clearance involves maintaining a low-pitch attitude early in the encounter, followed by a gradual pitch-up that ceases when the wind shear has been exited.

Nomenclature

D = airplane drag, lbf
E_s = specific energy, ft
$\mathcal{F}$ = F-factor
g = acceleration due to gravity, ft/s^2
h = altitude, ft
L = airplane lift, lbf
$\mathbf{L}$ = cost function Lagrangian or integrand
m = mass, slugs
q = pitch rate, rad/s (deg/s)
R = radius of downdraft column, ft
T = total engine thrust, lbf
t = time, s
U_{max} = maximum microburst horizontal wind speed, ft/s
$\boldsymbol{u}$ = control vector, q
V = airspeed, ft/s (kt)
W = weight, lbf
$\boldsymbol{w}$ = disturbance vector, $w_x w_h$
w_h = vertical wind speed, positive upward, ft/s (kt)
w_x = horizontal wind speed, tailwind positive, ft/s (kt)
x = horizontal distance over ground, ft
$\boldsymbol{x}$ = aircraft state vector, $xhV\gamma\alpha$
z_{max} = altitude of maximum outflow, ft
α = angle of attack, rad (deg)
γ = flight path angle with respect to air mass, rad (deg)
θ = pitch attitude, rad (deg)

Subscripts
f = final value
n = normalized quantity
0 = initial value

Presented as Paper 92-0730 at the AIAA 30th Aerospace Sciences Meeting and Exhibit, Reno, NV, Jan. 6–9, 1992; received March 17, 1992; revision received Aug. 17, 1992; accepted for publication Aug. 17, 1992.

*Research Assistant, Department of Mechanical and Aerospace Engineering. Student Member AIAA.

†Professor, Department of Mechanical and Aerospace Engineering. Associate Fellow AIAA.

Introduction

THE *Wind Shear Training Aid* published by the Federal Aviation Administration (FAA) recommends that upon encountering a severe wind shear, the pilot should apply full thrust and rotate the aircraft to an initial pitch target of 15 deg.[1] The objectives of the current work are to develop an analytical methodology for identifying a suitable target pitch angle (TPA) and to investigate the simulated recovery performance of propeller-driven commuter-type aircraft at the TPA. The applicability of the constant-pitch-attitude recovery to commuter-type aircraft is ascertained through comparison with results of deterministic trajectory optimization.

Low-altitude wind variability has long been recognized as a potential hazard to aircraft taking off or landing. During the period from 1964 to 1985, low-altitude wind shear was a contributing factor in at least 26 civil aviation accidents involving nearly 500 fatalities and over 200 injuries.[2] There is evidence to suggest that if undocumented close calls and incidents involving general aviation aircraft were included, these figures would be much higher. The FAA and the National Aeronautics and Space Administration (NASA) have established an integrated "wind shear program" to address the wind shear problem through focused research and development programs.[3] The objective of the program is to reduce the hazard of low-altitude wind shear to aircraft through the development of airborne and ground-based wind shear detection systems, crew alerting and flight management systems, and training and operating procedures.[4]

The most effective defense against the wind shear hazard is complete avoidance. In the event that avoidance is not possible, a suitable recovery technique must be applied to prevent a possible crash. As shown in Fig. 1, an airplane encountering a microburst wind shear typically encounters an increasing head wind first, improving the apparent performance of the aircraft. When faced with the headwind, the pilot may take action to prevent the airplane from climbing. In a microburst, this headwind disappears and is quickly followed by a downdraft and tailwind, whose performance-decreasing effects may easily exceed the climb and acceleration capabilities of the airplane. Ground impact may be unavoidable if a suitable recovery technique is not applied. The *Wind Shear Training Aid* recommends that on recognizing an encounter with severe wind shear, the pilot should command

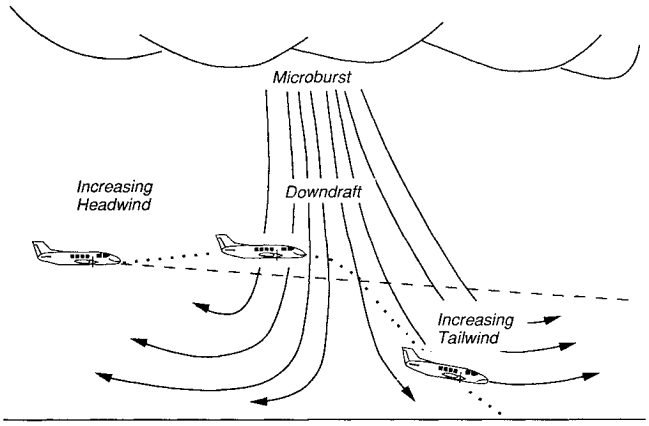

Fig. 1 Microburst encounter during approach to landing.

maximum thrust and rotate the aircraft to an initial TPA of 15 deg.[1] This pitch target was identified through rigorous analyses using full six degree-of freedom flight simulators and wind models representative of actual accident cases.[5]

The Training Aid was prepared primarily for the civil transport community, and it presents the material in the context of the operation of large jet transport (JT) aircraft. It has been recognized that general aviation and small commuter aircraft face no less a threat from wind shear than large jet transports. However, little research has been done to specifically address the issue of effective recovery techniques for the smaller aircraft. It has been shown that general aviation aircraft are intrinsically more vulnerable to the effects of microburst wind shear than jet transports.[6-8] AJT aircraft has a larger margin of trimmed airspeed above its 1g stall speed than a commuter aircraft, giving it a larger specific energy stored in this margin. This airspeed/energy margin gives the JT aircraft an advantage in both headwind/tailwind shears and downdrafts. A JT aircraft also has a much higher maximum rate of climb than a commuter aircraft, indicating that the JT's power plant is better able to make up for losses in specific excess power due to a wind shear condition. The objective of this study is to apply the FAA-recommended recovery strategy to a simulation model of a light, twin-reciprocating-engined commuter aircraft. The goals are to identify the factors influencing the choice of a suitable TPA and to assess the mert of the constant-pitch-attitude recovery as a whole through comparison with optimal trajectory analysis.

Effect of Wind Shear on Aircraft Performance

Point-Mass Equations of Motion

A point-mass model of the commuter aircraft is used for the present study. The coordinate system employed is presented in Fig. 2. The equations of motion under wind shear conditions are developed in Ref. 9, and repeated here. It is assumed that 1) the aircraft is a particle of constant mass, 2) flight takes place in a vertical plane, 3) Newton's law is valid in an Earth-fixed system, and 4) the wind flowfield is steady. With these premises, the equations of motion are

$$\dot{x} = V\cos\gamma + w_x \tag{1}$$

$$\dot{h} = V\sin\gamma + w_h \tag{2}$$

$$\dot{V} = (T/m)\cos\alpha - (D/m) - g\sin\gamma - \dot{w}_x\cos\gamma - \dot{w}_h\sin\gamma \tag{3}$$

$$\dot{\gamma} = (T/mV)\sin\alpha + (L/mV) - (g/V)\cos\gamma + (\dot{w}_x/V)\sin\gamma - (\dot{w}_h/V)\cos\gamma \tag{4}$$

$$\dot{\theta} = q \tag{5}$$

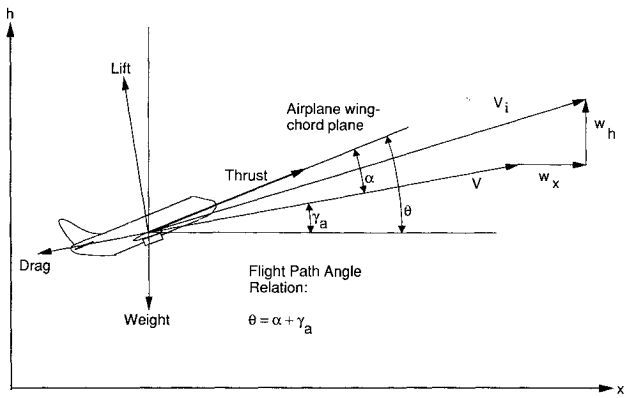

Fig. 2 Coordinate system.

where

$$\dot{w}_x = \frac{\partial w_x}{\partial x}\dot{x} + \frac{\partial w_x}{\partial h}\dot{h} + \frac{\partial w_x}{\partial t} \tag{6}$$

$$\dot{w}_h = \frac{\partial w_h}{\partial x}\dot{x} + \frac{\partial w_h}{\partial h}\dot{h} + \frac{\partial w_h}{\partial t} \tag{7}$$

The wind components in Eqs. (1) and (2), and the spatial shear terms in Eqs. (6) and (7) are obtained from the analytic microburst model used in the batch simulations.

Airplane Energy Concepts

The concept of total aircraft energy is useful for describing the impact of wind shear on airplane performance.[3] The total airplane energy is defined as the sum of the air-mass relative kinetic energy and the inertial potential energy. Kinetic energy is defined using the airspeed rather than the ground speed, since the airplane's ability to climb or maintain altitude depends on its speed with respect to the local air mass. The inertial potential energy is used because it is the altitude above ground that is useful to the airplane. The total energy per unit weight or "specific energy" is then defined as

$$E_s = (V^2/2g) + h \tag{8}$$

The rate of change of specific energy is given by

$$\dot{E}_s = \dot{V}(V/g) + \dot{h} \tag{9}$$

When combined with appropriate equations of aircraft motion, the energy rate is

$$\dot{E}_s = \left[\frac{T\cos\alpha - D}{W} - \left(\frac{\dot{w}_x}{g}\cos\gamma + \frac{\dot{w}_h}{g}\sin\gamma - \frac{w_h}{V}\right)\right]V \tag{10}$$

For representative numerical values of wind shear gradients and flight path angles typical of stabilized flight, the effect of wind shear can be accurately described by a nondimensional term known as the "F-factor," which is defined as

$$\mathcal{F} = (\dot{w}_x/g) - (w_h/V) \tag{11}$$

Equation (10) then takes the approximate form

$$\dot{E}_s = \{[(T - D)/W] - \mathcal{F}\}V \tag{12}$$

assuming $\cos\alpha \approx 1$. The time-rate-of-change of specific energy therefore depends linearly on a nondimensional parameter $\mathcal{F}$ that describes air mass movement. This parameter can be interpreted as the loss or gain in available excess thrust-to-weight ratio due to downdrafts, updrafts, and horizontal shears. A negative value of $\mathcal{F}$ indicates a performance *in-*

creasing situation for the airplane, while positive values indicate a performance *decreasing* situation. A persistent $\mathcal{F}$ of 0.15 effectively cancels the climb capability of most jet transports. If an aircraft encounters a wind shear condition that exceeds its climb capabilities, the airspeed margin above stall can be used to continue a climb or to arrest a descent. The flight management problem can then be considered a question of how best to distribute available aircraft energy over a microburst encounter.[10]

Simulation Model of Commuter Aircraft

The present study is concerned with the recovery performance of a light, twin-reciprocating engined commuter aircraft. The aerodynamic data for the aircraft were taken from a stimulation model developed at NASA Ames Research Center.[11] The aircraft has a gross weight of 6300 lb, and two 300 hp power plants. Lift and drag are modeled as functions of angle of attack, flap and gear deflection, and power setting. For the point-mass dynamics used, the control inputs were power setting and pitch rate. Pitch rate was limited to 3 deg/s for the simulated wind shear encounters, and negative pitch rates were generated as needed to prevent flight at angles of attack above stall warning. The commanded pitch rate was integrated directly to determine aircraft attitude. Engine dynamics were simulated using a first-order low-pass filter on the commanded power setting, with a time constant of 4 s.

Maximum Climb Capability in Wind Shear

The climb performance of the commuter aircraft in wind shear was first investigated by maximizing steady-state rate of climb as a function of an imposed $\mathcal{F}$. It was first assumed that $\mathcal{F}$ was due entirely to the horizontal shear effect, and second, that it was due entirely to the downdraft effect. Therefore, under the first assumption

$$\mathcal{F} = (\dot{w}_x/g) \tag{13}$$

and under the second assumption

$$\mathcal{F} = -\frac{w_h}{V} \tag{14}$$

Maximum steady-state rate of climb was computed as a function of $\mathcal{F}$ with the aircraft in approach configuration (45-deg flaps). Figures 3 and 4 indicate that the source of $\mathcal{F}$ has little effect upon the maximum rate of climb of which the aircraft is capable, but there is a substantial effect on the pitch attitude required to achieve it. The stronger the horizontal shear, the *lower* the pitch attitude is for maximum rate of climb. Conversely, the stronger the downdraft, the *higher* the pitch attitude is for maximum rate of climb. The results indicate that the most effective piloting technique depends on identifying the source of the threat to the aircraft.

An interesting summary of the aircraft's performance limits is presented in Table 1. The commuter aircraft can withstand

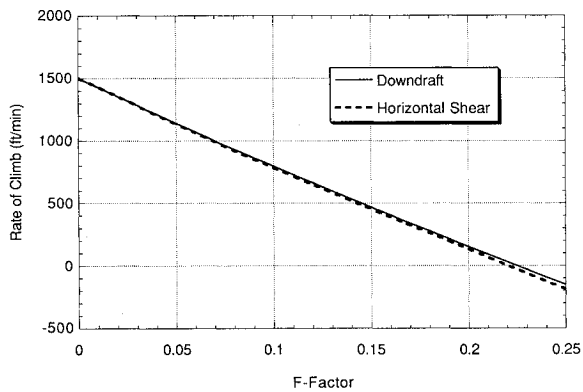

Fig. 3 Maximum rate of climb vs F-factor for a twin-engined commuter aircraft.

Table 1 Maximum horizontal shear and downdraft possible in level flight for a twin-engined commuter aircraft

Flap setting, deg	$\frac{\partial w_x}{\partial x_{max}}$, ft/s/ft	$w_{h_{max}}$, ft/s
0	0.061	16.5
45	0.069	13.6

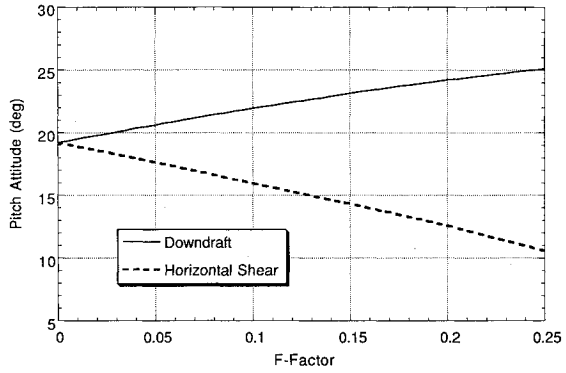

Fig. 4 Pitch attitude for maximum rate of climb vs F-factor.

more of a downdraft in level flight with flaps retracted before its climb capability is overcome, and more of a horizontal shear with 45-deg flaps. This implies that if the nature of the atmospheric disturbance affecting the aircraft can be accurately identified, flaps could be used to elicit additional climb performance from the vehicle. It may not be desirable to adjust flaps during a manual recovery due to the increased pilot work load, but an automated recovery control system might be able to take advantage of the effects of flap setting on climb performance.

Batch Simulation of Microburst Encounters

The analysis of static climb performance under conditions of wind shear indicates that any single TPA is a compromise between the distinct effects of horizontal shear and downdraft. The nature of this tradeoff was ascertained by simulating the recovery performance of the aircraft through an analytic downburst model developed at NASA Langley Research Center.[12] The model represents an axisymmetric stagnation point flow, based on wind velocity profiles from the Terminal Area Stimulation System (TASS). Simulation of microbursts of different size and strength is possible through specification of the radius of the downdraft column, the maximum horizontal wind speed, and the altitude of maximum outflow. Wind velocity components and spatial gradients required for integrating the equations of motion [Eqs. (1–7)] are obtained directly from the wind model. The aircraft equations of motion were integrated using a second-order Runge-Kutta scheme with a timestep of 0.05 s.

Encounters During Approach to Landing

The effect of downburst strength during approach encounters was investigated by placing the aircraft at a distance of 10,000 ft from the microburst core at initial altitudes ranging from 600 to 1400 ft. The aircraft was initialized on the glide slope in approach configuration; 45-deg flaps, 95-kt airspeed. It tracked the glide slope until $\mathcal{F}$ exceeded 0.1, at which point a specified recovery target pitch angle was commanded. Instantaneous detection of the F-factor "hit" was assumed. The encounter was considered complete as soon as a sustained positive climb rate was established. Simulation results are summarized in Figs. 5 and 6. In Fig. 5, minimum altitude during the encounter is plotted against TPA and initial altitude for a microburst of fixed size and strength. Figure 6 presents minimum altitude against TPA and maximum horizontal wind speed for a given initial altitude and microburst radius.

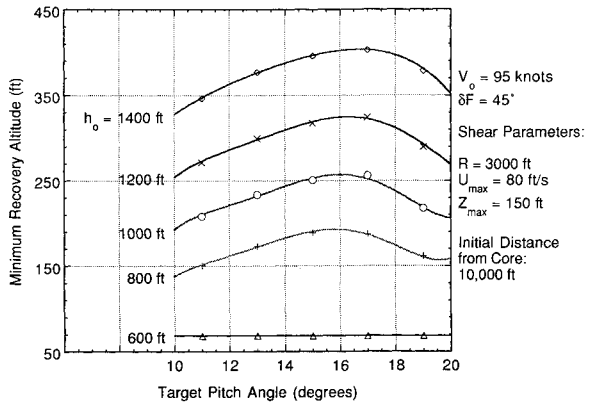

Fig. 5 Minimum recovery altitude vs target pitch angle and initial altitude; approach encounters.

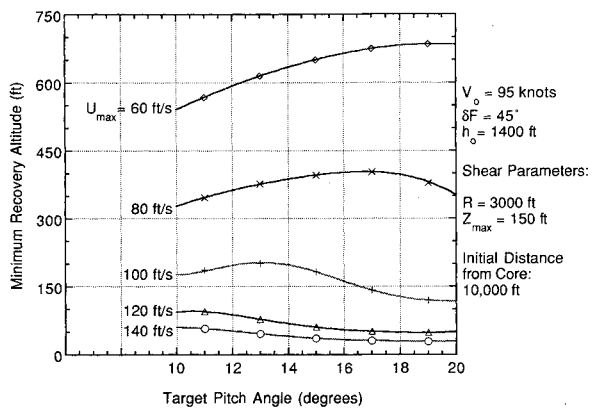

Fig. 6 Minimum recovery altitude vs target pitch angle for a range of maximum outflow velocities.

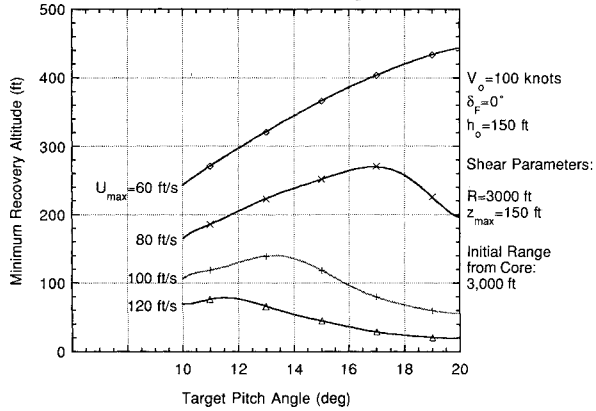

Fig. 7 Minimum recovery altitude vs target pitch angle and maximum outflow; takeoff encounters.

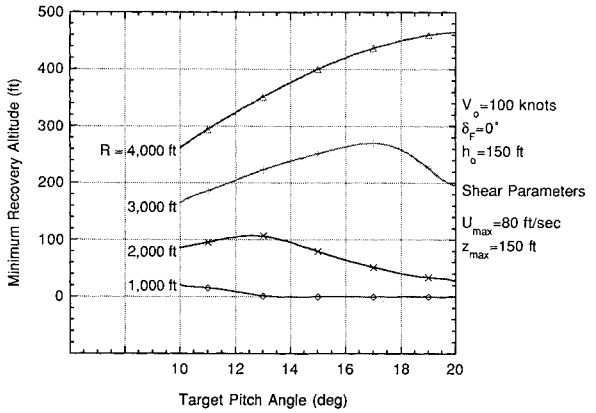

Fig. 8 Minimum recovery altitude vs target pitch angle and microburst radius; takeoff encounters.

It is apparent from the simulation results that no single pitch attitude stands out over all of the different encounters. In all cases, as the TPA increases beyond the value that maximizes ground clearance, the aircraft experiences prolonged periods at or above stall-warning angle of attack. As the altitude of the encounter is reduced, the pitch attitude that maximizes ground clearance becomes smaller. This result is consistent with the earlier observation that in horizontal shears, better climb performance is achieved at lower pitch attitudes. In a relatively low-altitude encounter, the horizontal shear might be expected to have a greater effect than the downdraft, as strong downdrafts are not likely to exist very close to the ground. Consequently, recoveries at lower target pitch angles would be better for low-altitude encounters. As the strength of the shear increases (through U_{max}), the target pitch angle to maximize ground clearance drops substantially.

Takeoff Encounters

The effect of microburst strength on recovery performance during takeoff encounters was also investigated. The aircraft was initialized in a nominal initial climb configuration: flaps retracted, 100-kt airspeed, 1000 ft/min rate of climb. Pitch and thrust inputs were generated as necessary to maintain the nominal climb rate and airspeed until $\mathcal{F}$ exceeded 0.1, at which point a specified TPA was commanded. Simulation results are summarized in Fig. 7. Minimum recovery altitude is presented against TPA and U_{max}, for a given initial position relative to the downburst core. The results are similar to those for the approach encounters: as the microburst becomes stronger, the target pitch angle for best recovery performance becomes smaller. The effect of microburst size for a given divergence (i.e., a fixed U_{max}) is illustrated in Fig. 8. As the microburst is made smaller in radius, the target pitch angle that maximizes the recovery altitude becomes smaller. In these cases, the aircraft was initialized in a nominal climb-out at an initial distance from the core equal to the microburst radius R. Thus, as R is increased, the aircraft is exposed to a given horizontal wind speed change over a larger distance.

Selection of the Target Pitch Angle

The investigation of static climb performance in wind shear and the batch simulations of microburst encounters hve shown that there is no single TPA that stands out as being the most effective. Any single figure is a compromise between the distinct effects of downdraft and horizontal shears. In relatively weak microbursts, best performance is obtained at quite high TPAs (as much as 20 deg in some cases). In severe microburst encounters at very low altitudes, low TPAs (10–12 deg) are preferable. If high TPAs are used in the very severe wind shear encounters, the aircraft experiences long periods at stall warning and degraded recovery performance. These results make it difficult to justify any one TPA over another from the standpoint of recovery performance. While a microburst that is best traversed using a 20-deg TPA might be too weak to be considered representative of hazardous wind shear, a microburst that requires the use of a 10-deg TPA might be unduly severe. If a single TPA is to be defined for both approach and takeoff encounters, it will be necessary to evaluate recovery performance in several different microbursts containing realistic wind profiles. The parameter sets for nine such microbursts were found in Ref. 13, and are shown in Table 2. The parameters are based on data from the TASS,[14] which is a time-dependent multidimensional model of cloud physics.

Recovery performance was evaluated through each of these microbursts for approach and takeoff encounters at various initial ranges and altitudes. As shown by Bowles[3] and others, maximum horizontal wind speed change divided by the corresponding distance (i.e., U_{max}/R) is a good indicator of wind shear severity. By this measure, microbursts nos. 1, 2, and 9

Table 2 TASS microburst parameter sets for evaluation of target pitch angle

Microburst	Radius, ft	U_{max}, ft/s	z_{max}, ft	U_{max}/R
1	920	37.0	98	0.0402
2	1180	47.6	98	0.0403
3	2070	58.4	131	0.0282
4	4430	68.9	164	0.0155
5	3450	88.2	197	0.0256
6	3180	53.1	262	0.0167
7	1640	46.0	164	0.0280
8	5250	81.3	197	0.0155
9	1250	67.6	100	0.0541

Table 3 Additional severe microburst parameter sets

Microburst	Radius, ft	U_{max}, ft/s	z_{max}, ft	U_{max}/R
10	2000	60.0	150	0.0300
11	2000	80.0	150	0.0400
12	3000	80.0	150	0.0267
13	3000	100.0	150	0.0333
14	3000	120.0	150	0.0400
15	4000	100.0	150	0.0250
16	4000	110.0	150	0.0275
17	4000	120.0	150	0.0300

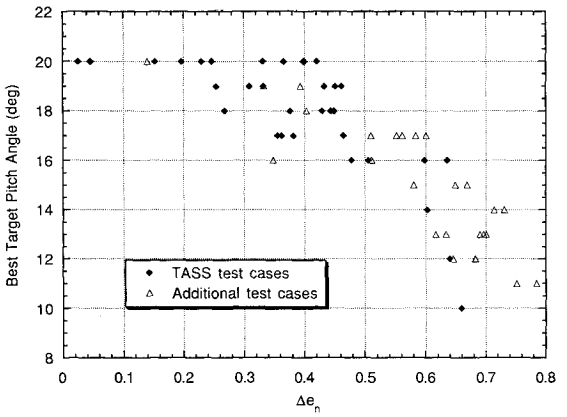

Fig. 9 Target pitch angle for best recovery performance vs normalized energy loss; approach encounters.

are the most severe. An additional set of parameters were defined to study recovery performance in equally severe microbursts of different size. The parameters for these microbursts are shown in Table 3.

The aircraft total energy concept is very useful in interpreting the simulation results, which are summarized in Figs. 9 and 10. Let E_0 be the aircraft energy at the instant that the recovery is initiated:

$$E_0 = \frac{V^2}{2g} + h \Big|_{\mathcal{F}=0.1} \tag{15}$$

Let E_{min} be the minimum energy during the encounter:

$$E_{min} = \min_t \left[\frac{V(t)^2}{2g} + h(t) \right] \quad t_0 \le t \le t_f \tag{16}$$

Finally, define the "normalized energy loss" as

$$\Delta e_n = [(E_0 - E_{min})/E_0] \tag{17}$$

In Figs. 9 and 10, the TPA for the best recovery performance (as measured by ground clearance) is plotted against normalized energy loss. The results from the TASS wind profiles are separated from the additional severe microburst cases. For most of the TASS cases, high TPAs (16–20 deg) seem to be the most effective for both takeoff and approach encounters. The only TASS wind profile where a TPA less than 16 deg was the most effective was microburst no. 9, which had the highest mean shear (U_{max}/R) of all microbursts considered. If microbursts 1–9 are representative of what the aircraft might realistically encounter, a TPA between 16–20 deg may be preferable on average to the FAA recommended 15 deg. As a practical matter though, it would be preferable to use a TPA that is marked distinctly on the attitude indicator. As such, a TPA of 17.5 deg may be reasonable for this commuter aircraft.

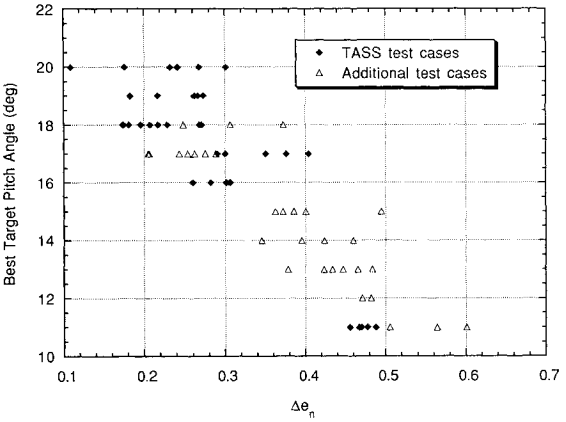

Fig. 10 Target pitch angle for best recovery performance vs normalized energy loss; takeoff encounters.

When the additional severe wind profiles are considered, an interesting trend is evident. As the normalized energy loss Δe_n increases, the most effective TPA tends to become smaller. The spread in the results is very likely due to the proportions of energy loss arising from downdraft and horizontal shear. This result again illustrates the nature of the compromise imposed by a single TPA. However, it does have interesting implications for the application of forward-looking sensor technology. If such a device could make a reasonable estimate of the anticipated energy loss through a wind shear, it could provide flight guidance to the pilot to a pitch attitude that makes better use of aircraft energy than a single fixed TPA. For a given anticipated energy loss, the most effective TPA would depend on the initial energy state of the airplane: the faster the aircraft is going (or the higher it is), the higher the preferred TPA.

Optimal Trajectories Through Wind Shear

The overall merit of the constant pitch attitude recovery for the commuter aircraft remains uncertain. It is not at all clear that maintaining a constant pitch attitude is the most effective means of recovering from a microburst wind shear. Miele[15] has found that for a jet transport aircraft, an optimal means of recovering from a microburst during an approach encounter involves the use of relatively low pitch attitudes very early in the encounter, followed by a gradual pitch-up that ceases near the core of the microburst. The resultant performance is superior to that offered by a constant pitch attitude strategy. This issue was explored for the commuter aircraft by comparing some of the target pitch angle recoveries to optimal trajectories through the same wind field. Optimal trajectories were computed for microburst encounters during approach to landing.

The purpose of trajectory optimization is to determine a control history $\boldsymbol{u}^*(t)$ that minimizes a cost function.[16] The cost function considered here consists of two parts: 1) a scalar integral function of the state and control, and 2) a scalar algebraic function of the final state:

$$J = \Phi[\boldsymbol{x}(t_f)] + \int_{t_0}^{t_f} \mathbf{L}[\boldsymbol{x}(t), \boldsymbol{u}(t), \boldsymbol{w}(t), t]\, dt \tag{18}$$

The choice of the Lagrangian $\mathbf{L}[\cdot]$ and the final state penalty $\Phi[\cdot]$ determines the nature of the optimizing solution. The optimal control history $\boldsymbol{u}^*(t)$ acts on the dynamic system, whose trajectory is determined by integrating the ordinary differential equation

$$\dot{\boldsymbol{x}} = f[\boldsymbol{x}(t), \boldsymbol{u}(t), \boldsymbol{w}(t), t] \tag{19}$$

$$\boldsymbol{x}(t_0) = \boldsymbol{x}_0 \tag{20}$$

The dynamic system equations are those of point-mass aircraft motion, Eqs. (1–7). Power was held at maximum throughout the optimal trajectory, so that the only element of the control vector $\boldsymbol{u}(t)$ was the pitch rate of the aircraft. The objective of the optimization was to minimize the peak altitude loss during the microburst encounter, using a cost function similar to that employed by Miele and Wang[15]:

$$\min I = \max_t[h_{\text{ref}} - h(t)] \qquad t_0 \le t \le t_f \tag{21}$$

Stated another way, the goal is to minimize the peak difference between a constant reference altitude and the instantaneous altitude. This is equivalent to maximizing the minimum altitude. Equation (21) describes a minimax or Chebyshev problem of optimal control. As shown by Miele, it can be reformulated as a Bolza problem of optimal control [Eq. (18)], where one minimizes the integral cost function

$$J = \int_{t_0}^{t_f} [h_{\text{ref}} - h(t)]^p \, dt \tag{22}$$

and p is a large even positive integer. A value of $p = 8$ was used for this study. The cost function Lagrangian and terminal penalty used took the form

$$\mathbf{L}(\boldsymbol{x}, \boldsymbol{u}) = k_h[h(t) - h_{\text{ref}}]^8 + k_v[V(t) - V_{\text{ref}}]^2 + k_q q(t)^2 + \mathbf{L}_\alpha[\alpha(t)] + \mathbf{L}_q[q(t)] \tag{23}$$

$$\Phi[\boldsymbol{x}(t_f)] = k_\gamma[\gamma(t_f) - \gamma_{\text{ref}}]^2 \tag{24}$$

The constants k_h, k_v, k_q, and k_γ are used to scale the contribution of each term to the cost function. The reference flight path angle γ_{ref} for the terminal penalty was that for best rate of climb in still air, which was 11.7 deg for the commuter in approach configuration. The incremental cost functions $\mathbf{L}_\alpha$ and $\mathbf{L}_q$ were added as "soft constraints" to prevent flight at angles of attack above stall warning, and to limit the pitch rate of the aircraft to the range ± 3 deg/s. Each of these functions remains zero, provided that their respective arguments do not violate certain limits. Once a particular limit is exceeded, the contribution to the Lagrangian grows quadratically with the magnitude of the violation. Thus

$$\boldsymbol{L}_\alpha[\alpha(t)] = \begin{cases} k_\alpha[\alpha(t) - \alpha_{\max}]^2 & \alpha > \alpha_{\max} \\ 0 & \alpha \le \alpha_{\max} \end{cases} \tag{25}$$

$$\mathbf{L}_q[q(t)] = \begin{cases} k_{q2}[q(t) - q_{\max}]^2 & q > q_{\max} \\ 0 & q_{\min} \le q \le q_{\max} \\ k_{q2}[q(t) - q_{\min}]^2 & q < q_{\min} \end{cases} \tag{26}$$

The limits were set in Table 4.

Table 4 Thresholds for soft constraint functions

Variable	Value
$a_{\max}$	12 deg
$q_{\max}$	3 deg/s
$q_{\min}$	−3 deg/s

Computation of Optimal Trajectories

Optimal trajectories were calculated for microburst encounters during approach to landing. A conjugate gradient method[17] was used to minimize Eq. (18) with the cost function Lagrangian and terminal penalty function specified by Eqs. (23) and (24). The nominal state and control histories used to initiate the numerical iteration were those of a TPA recovery. The initial time t_0 for the optimal trajectory was the instant that $\mathcal{F}$ exceeded 0.1, while the final time t_f was the same as that of the TPA recovery. The constant h_{ref} in Eq. (23) was defined as the altitude at which $\mathcal{F}$ exceeded 0.1. Thus, the optimal trajectory defines the "best" way to recover from the microburst, given that it has been penetrated. Inspection of the pitch attitude history $\theta(t)$ for $t_0 \le t \le t_f$ provides insight into the nature of the most effective piloting technique for maximizing ground clearance.

Altitude and pitch attitude histories for a particular TPA and optimal recovery are presented in Figs. 11 and 12. The parameters of the test case are as follows:

R, ft	3,000
$U_{\max}$	80
$z_{\max}$	150
Initial altitude, ft	1,400
Initial range from microburst core, ft	10,000

The recovery procedure was initiated approximately 47 s into the encounter. Ground clearance was maximized at a TPA of 17 deg for this particular microburst. Note that 17 deg is not necessarily the suggested TPA for the commuter; it was the most effective for this microburst encounter. It is evident from the optimal trajectory that the 17-deg TPA recovery does not take full advantage of the aircraft's available performance. At the instant that the aircraft established a positive climb rate in the optimal maneuver (at $t = 85$ s), it still would be descending at about 800 ft/min, had it executed a constant

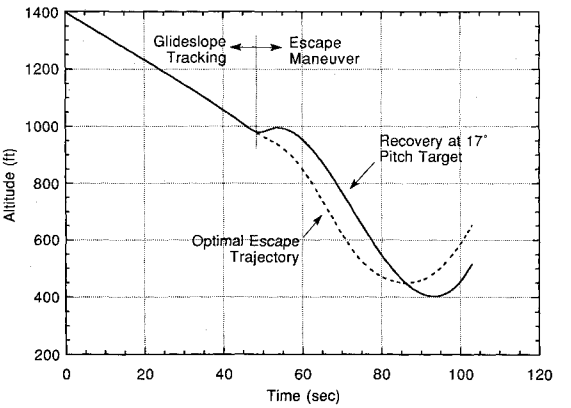

Fig. 11 Altitude vs time for target pitch angle and optimal recovery.

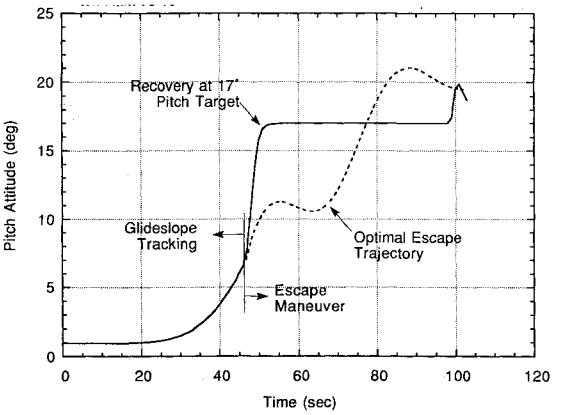

Fig. 12 Pitch attitude vs time for target pitch angle and optimal recovery.

Table 5 Comparison of TPA and optimal recovery

	TPA recovery	Optimal recovery
Minimum altitude, ft	403	455
Minimum total energy, ft	596	630
Minimum airspeed, kt	65	63
Maximum angle of attack, deg	10.8	9.3

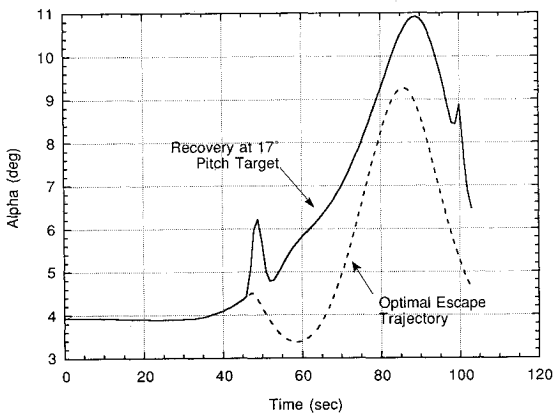

Fig. 13 Angle of attack vs time for target pitch angle and optimal recovery.

pitch attitude recovery. Qualitatively, the optimal recovery involves maintaining a relatively low pitch attitude (about 11 deg) early in the encounter, followed by a gradual pitch-up to about 20 deg by the end of the microburst. The low pitch attitude early in the encounter has the effect of preserving kinetic energy, which is later traded for climb rate. Salient features of the TPA and optimal recovery are compared in Table 5.

When excecuting the optimal maneuver, the aircraft recovers at a higher altitude and with a higher minimum total specific energy. In addition, the aircraft is exposed to generally lower angles of attack, as seen in Fig. 13. It should be noted that the performance attained using the optimal technique can only be approximated in practice, since global knowledge of the flowfield is required for optimization. Other researchers[9,18] have developed nonlinear feedback control laws for a jet transport aircraft that provide near-optimal recovery performance in downbursts. These feedback laws require only local knowledge of the flowfield about the aircraft. Although not pursued here, such feedback laws could be developed for a commuter-type aircraft to provide recovery performance better than that offered by the constant pitch attitude strategy. For example, feedback of w_h and $\dot{w}_x$ could be used to compute a pitch attitude that is most suited to dealing with the atmospheric disturbance at hand.

Conclusions

The optimal trajectory indicates that a constant pitch attitude recovery is not the most effective strategy in a wind shear encounter during approach to landing; however, given the simplicity of the technique, it is a reasonable recovery maneuver. A superior strategy might be a piecewise-constant pitch attitude recovery that better approximates the optimal technique. The analysis of aircraft climb and recovery performance has shown that the most effective TPA depends at the very least on the nature of the energy hit to the aircraft, the size and strength of the microburst, and the aircraft's initial position with respect to the downburst core. Analysis of the simulated encounters through the TASS wind profiles and the additional severe microbursts leads to two conclusions: The commuter aircraft under consideration might do better on average at a TPA of 17.5 deg than at the *Wind Shear Training Aid's* suggested 15 deg. Also, as the aircraft's normalized energy loss through a microburst increases, the most effective TPA generally becomes smaller.

This study considered flight directly through the microburst core; an aircraft penetrating a microburst away from the core probably would experience diminished longitudinal wind components as well as upsetting lateral moments that would have an effect on recovery performance at a particular TPA. The crosswind components in such a case would complicate the piloting task of maintaining a particular pitch attitude, and they deserve further study.

Acknowledgments

This research has been sponsored by the FAA and the NASA Langley Research Center under Grant NGL 31-001-252.

References

[1]*Windshear Training Aid*, U.S. Dept. of Transportation, Federal Aviation Administration, Washington, DC, 1987.

[2]Townsend, J., "Low-Altitude Wind Shear and Its Hazard to Aviation," National Academy Press, Washington, DC, 1983.

[3]Bowles, R. L., "Reducing Windshear Risk Through Airborne Systems Technology," 17th Congress of the International Council of the Aeronautical Sciences, Stockholm, Sweden, 1990.

[4]Hinton, D. A., "Piloted-Simulation Evaluation of Recovery Guidance for Microburst Wind Shear Encounters," NASA TP 2886, Washington, DC, 1989.

[5]Kupcis, E. A., "Manually Flown Windshear Recovery Technique," *Proceedings of the 29th Conference on Decision and Control*, Honolulu, HI, Dec. 1990, pp. 758, 759.

[6]Psiaki, M. L., "Control of Flight Through Microburst Wind Shear Using Deterministic Trajectory Optimization," Ph.D. Dissertation, Princeton Univ., Rept. 1787-T, Princeton, NJ, 1987.

[7]Psiaki, M. L., and Stengel, R. F., "Optimal Aircraft Performance During Microburst Encounter," *Journal of Guidance, Control, and Dynamics*, Vol. 14, No. 2, 1991, pp. 440–446.

[8]Psiaki, M. L., and Stengel, R. F., "Analysis of Aircraft Control Strategies for Microburst Encounter," *Journal of Guidance, Control, and Dynamics*, Vol. 8, No. 5, 1985, pp. 553–559.

[9]Miele, A., Wang, T., and Melvin, W., "Optimal Take-Off Trajectories in the Presence of Windshear," *Journal of Optimization Theory and Applications*, Vol. 49, No. 1, 1986, pp. 1–45.

[10]Hinton, D. A., "Flight Management Strategies for Escape from Microburst Encounters," NASA TM 4057, Washington, DC, 1988.

[11]Hoh, R., Mitchell, D., and Myers, T., "Simulation Model of Cessna 402B," NASA Ames Research Center, NASA CR-152176, Moffett Field, CA, July 1978.

[12]Oseguera, R. M., and Bowles, R. L., "A Simple, Analytic 3-Dimensional Downburst Model Based on Boundary Layer Stagnation Flow," NASA TM 100632, Washington, DC, July 1988.

[13]"Airborne Windshear Warning and Escape Guidance Systems for Transport Airplanes," Federal Aviation Administration, TSO-C1117, Dept. of Transportation, Washington, DC, 1990.

[14]Byrd, G. P., Proctor, F. H., and Bowles, R. L., "Evaluation of a Technique to Quantify Microburst Windshear Hazard Potential to Aircraft," *Proceedings of the 29th IEEE Conference on Decision and Control*, Honolulu, HI, Dec. 1990, pp. 689–694.

[15]Miele, A., Wang, T., Tzeng, C., and Melvin, W.,"Optimization and Guidance of Abort Landing Trajectories in a Windshear," *Proceedings of the AIAA Guidance, Navigation, and Control Conference*, Monterey, CA, Aug. 1987, pp. 483–509.

[16]Stengel, R. F., *Stochastic Optimal Control: Theory and Application*, Wiley-Interscience, New York, 1986.

[17]Bryson, A. E., Jr., and Ho, Y. C., *Applied Optimal Control*, Hemisphere, Washington, DC, 1975.

[18]Zhao, Y., and Bryson, A. E., Jr., "Control of an Aircraft in Downbursts," *Journal of Guidance, Control, and Dynamics*, Vol. 13, No. 5, 1990, p. 819.